Physical characterization of NEA Large Super-Fast Rotator (436724) 2011 UW158

XIII Congresso Italiano di Planetologia, Bormio 21-26 Febbraio 2016

A. Carbognani[1], B. L. Gary[2], J. Oey[3], G. Baj[4], P. Bacci[5]

[1]Astronomical Observatory of the Autonomous Region of Aosta Valley (OAVdA), Aosta - Italy ,
[2]Hereford Arizona Observatory (U.S.A.), [3]Blue Mountains Observatory (Australia),
[4]Astronomical Station of Monteviasco (Italy), [5]Astronomical Observatory of San Marcello Pistoiese (Italy)

Introduction

The near-Earth asteroid (436724) 2011 UW158 was discovered on 2011 Oct 25 by the Pan-STARRS observatory at Haleakala (Hawaii, U.S.A.). This object has a relatively low delta-V for spacecraft missions (11.96 km/s) and is on NASA's Near-Earth Object Human Accessible Targets Study list. A fly-by with the Earth occurred on 2015 Jul 19 at 0.0164 A.U. so 2011 UW158 also became a radar target for Goldstone, Arecibo and Green Bank (Naidu et al., 2015). This asteroid was followed by an international team of optical observers (see Table I) on 31 nights between 2015 Jun 17 and Sept 26. A phase curve slope of 0.023 ± 0.001 mag/deg was determined for a phase angle range of 17 to 90 deg. This slope is used to estimate geometric albedo = 39 ± 9 %, absolute magnitude H = 19.93 ± 0.11 mag, and diameter = 220 ± 40 m. Combining the collected photometric data using the standard lightcurve inversion method, we obtain a unique spin axis solution with ecliptic coordinates $\lambda = 290° \pm 3°$, $\beta = -39° \pm 2°$, a sidereal period $P_S = 0.610752 \pm 0.000001$ h and a shape model qualitatively consistent with radar observations.

Observer	Telescope	CCD camera
Bacci	Ref. 0.60-m f/4	Apogee Alta 1024
Baj	RC 0.25-m f/8	SBIG-ST10
Carbognani	RC 0.81-m f/7.9	FLI 1001E
Gary	SC 0.35-m f/10	SBIG-ST10XME
Oey	CDK 0.61-m f/6.8	Apogee U42

Table I - Observers, telescopes and CCD camera used for 2011 UW158.

The Cohesionless Spin-Barrier

Asteroids of size D ≥ 0.15 km generally do not have periods P ≤ 2.2 h, a limit known as the *cohesionless spin-barrier* (Fig. 1). This barrier can be explained by the rubble-pile structure model (Pravec and Harris 2000). The exceptions to this "rule," called large super-fast rotators (LSFRs), are very few; 2001 OE84, (335433) 2005 UW163, and 2011 XA3 are the best known examples. The presence of these objects was theorized for the first time by Holsapple (2007). These results have been confirmed and enriched by subsequent theoretical studies, such as by Sànchez and Scheeres (2014), in which a model for the origin of the cohesion forces within a regolith has been proposed. The presence of cohesion forces begins to be important only for objects with diameter D < 10 km. So, for small bodies (0.15 km < D <10 km) with rubble-pile structure, the presence of even a very small amount of strength allows much more rapid spin than the simple cohesionless spin-barrier value.

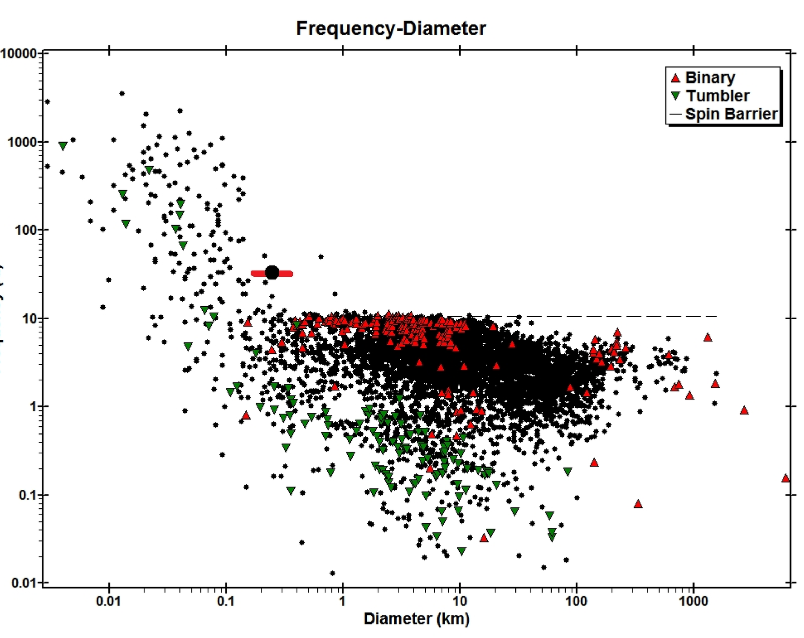

Figure 1 - Plot of asteroid spin rate vs. diameter (from IAU Minor Planet Data Center). The horizontal dashed line is the "cohesionless spin-barrier". NEA 2011 UW158 is shown as a large black dot, within a red rectangle representing a range of effective optical diameters corresponding to the smallest to the largest dimension. The radar effective diameter is slightly larger by a factor of about 1.7.

Lightcurve and Rotation Period

The asteroid 2011 UW158 was first observed by Gary with unfiltered CCD images calibrated using r'-mag's of APASS stars in the UCAC4 catalog (Gary, 2016). Thanks to these first observations a synodic rotation period of only 36.66 minutes was first found by Gary on 2015 Jun 17 and independently by Oey on Jul 1 (Fig. 2). After the discovery of the fast rotation period one key question became "Is the effective diameter really > 0.15 km?". This goal was the Gary's motivation for creating a phase curve that could be used to evaluate absolute magnitude H_v and geometric albedo ρ_v. The phase curve model of Belskaya and Schevchenko (2000), hereafter B&S, was adopted for this work.

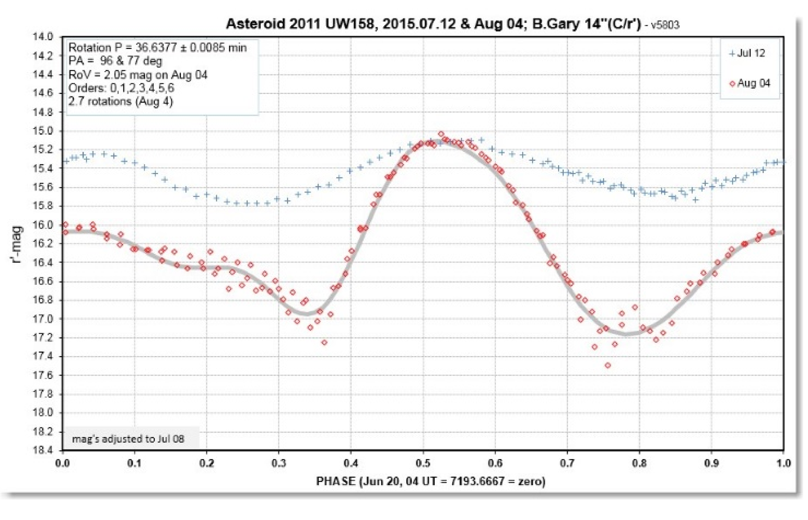

Figure 2 - Phase-folded lightcurve for two dates, showing change in amplitude and shape. The r'-mags have been adjusted to a standard date (Jul 08) using an HG model with G = 0.15 to help in detecting which parts of the rotation have undergone change (Gary, 2016).

Phase Curve, Albedo and Size

In the B&S work, they analyzed 33 well-studied main belt asteroids using a 3-term phase effect model first introduced by Schevchenko (1997):

$$V(\alpha) = V_o + b \times \alpha - a/(1+\alpha) \qquad (1)$$

where V(α) is V-mag at phase angle α (the arc subtended by the directions to the observer and to the Sun as measured from the observed body), Vo is V-mag at zero phase, "b" is phase coefficient (a slope term) fitted to V(α) measurements and "a" is an "opposition effect" (OE) amplitude term. B&S found that there was a strong correlation between the phase coefficient "b" and albedo, and also an inverted U-shape relationship between the OE amplitude term "a" and albedo. Their equation relating phase coefficient "b" and V-mag albedo at α = 0, ρ_v, is:

$$b = 0.013 - 0.024 \times \log(\rho_v) \qquad (2)$$

where "b" has units of mag/deg and ρ_v is fractional geometric albedo. The B&S model has a straight line slope parameter b = 0.0228 ± 0.0008 mag/deg. Substituting this b value in the above equation (2) yields geometric albedo $\rho_v = 39 \pm 9$ %. Since information for α close to zero is not present the size of OE isn't measured. We shall use the B&S relation between OE and albedo. For an albedo of 39% they find that the OE term a = 0.29 ± 0.02 mag. The solid trace in Fig. 3 includes the OE component. The B&S model fit has r'-mag = 19.70 ± 0.05 at α = 0. Converting to V-mag yields 19.93 ± 0.11, which corresponds to nominal H_v value. Asteroid size can now be calculated using the standard equation (Harris, 1997):

$$D\,[km] = (1329 / \mathrm{sqrt}(\rho_v)) \times 10^{-0.2 \times Hv} \qquad (3)$$

Setting $H_v = 19.93 \pm 0.11$ mag and $\rho_v = 0.39 \pm 0.09$, yields an equivalent diameter D = 220 ± 40 m. The visible extents of the asteroid in the radar images suggest an elongated object with dimensions of about 600 x 300 m (Naidu et al., 2015) so with an effective diameter of about 380 m, larger than optical observations. With this diameter value coupled with the fast rotation period, 2011 UW158 result a good candidate LSFR asteroids (see Fig. 1).

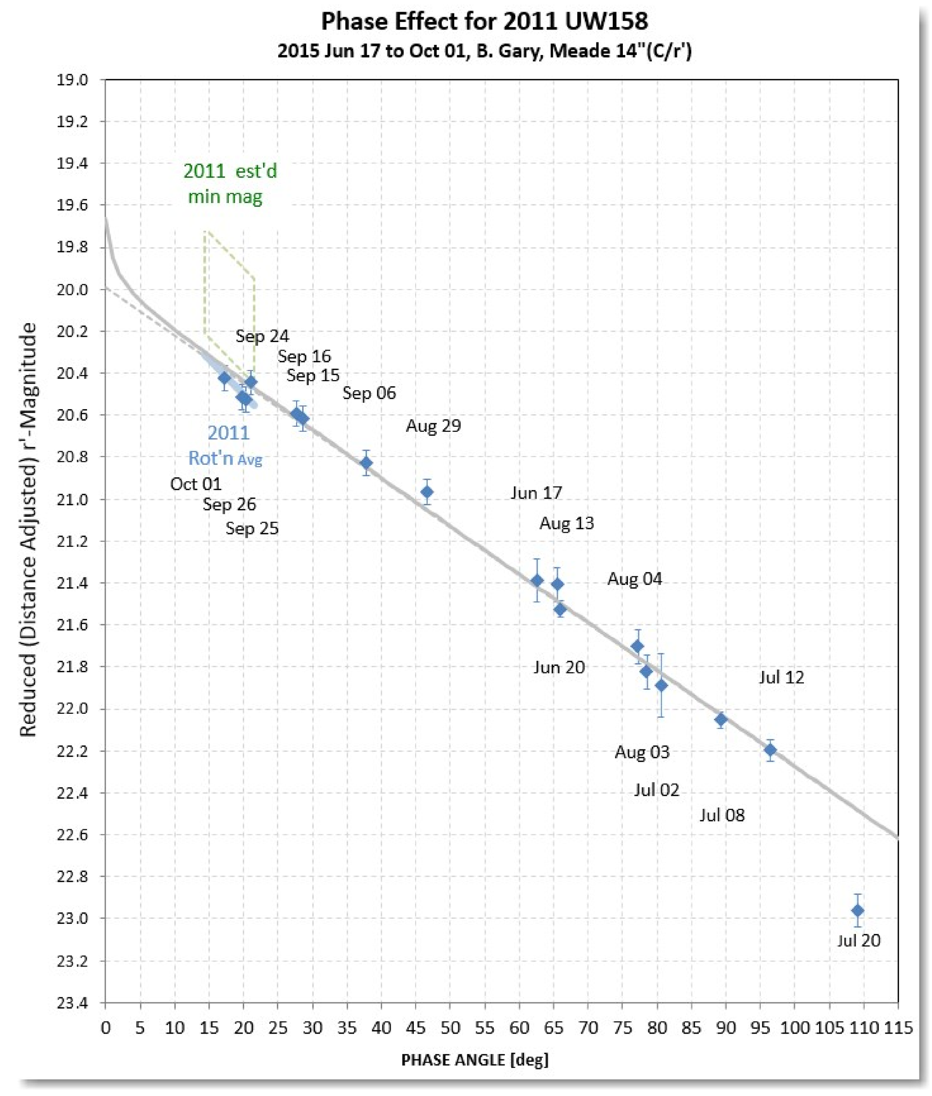

Figure 3 - The B&S model fit. Observing date annotations are included (Gary, 2016).

Pole Search

Our purpose was also to determine the pole of rotation and convex shape using the standard lightcurve (LC) inversion method (Kaasalainen et al. 2001; Kaasalainen and Torppa, 2001). In most cases, it is not possible to get a reasonable solution for a pole using LC inversion with photometric observations from one apparition. In our case the range of observed phase angle is 62° to 109° and 109° to 20° while the amplitudes of angle bisector are ΔLPAB = 137° and ΔBPAB = 64°, sufficiently broad for trying to determine pole orientation and shape (Fig. 4). The LC inversion process was performed using MPO LCInvert v11.1.0.2 (Bdw Publishing), which implements the core algorithms developed by Kaasalainen and then converted to C language by Josef Durech.

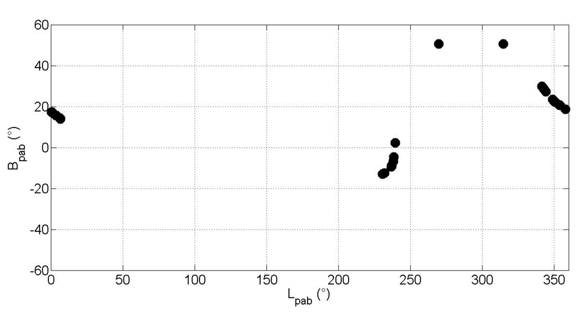

Figure 4 - Distribution of phase angle bisector (PAB) for 2011 UW158.

The inversion process started by finding the sidereal rotation period of the asteroid (Carbognani et al., 2016). A search in MPO LCInvert was confined to 0.6100 to 0.6115 h, a range that includes the synodic period found in the single phased LC, with weight 0.5. However, inclusion of all observations leads to χ^2 values that are quite high. After some tests, we found that by restricting observations to those by Gary (in this way the range of the phase angle remains unchanged) and those before Aug 15 for the other observers, the χ^2 values were reduced to reasonable values. The search process found an isolated, deep, and flat minimum in the plot of χ^2 vs. sidereal period (Fig. 5). A renormalization was not necessary since reduced $\chi^2 \sim 1.0$ (i.e., N = 24 and sum χ^2 is also ~24). The minimum appears asymmetrical, i.e. the descending branch is less steep than the ascending branch. For this reason we assumed the value of the point to the right, 0.6107643 h, for the starting period in the pole search.

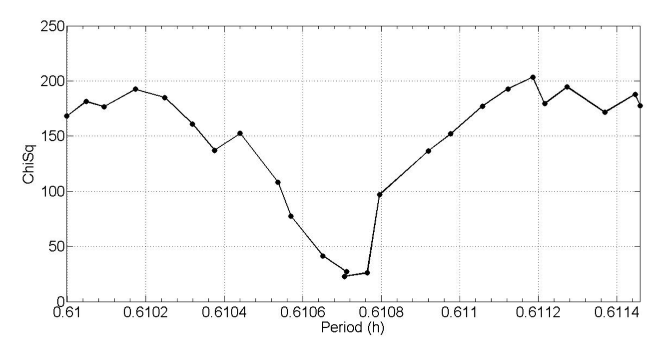

Figure 5 - ChiSq vs period for 2011 UW158 (Carbognani et al., 2016).

For the pole orientation search, we started using the "Medium" search option in LCInvert (312 fixed pole positions with 15° longitude-latitude steps). The previously found sidereal period was set to "float" and the weight parameter = 0.8. The pole search found one cluster of solutions centered around ecliptic coordinates λ = 285° and β = –45° with a sidereal period P = 0.61075717 h. Fig. 6 shows the distribution of log(χ^2) values. A final search for a spin axis solution was made using the lowest value in this island. Here the longitude and latitude are allowed to float, as was the period. The spin axis parameters were then used to generate a final shape and spin axis model. Refining the pole search, using the "Fine" option of LCInvert software (49 fixed pole steps with 10° longitude-latitude pairs) and the previous period/longitude/latitude set to "float", we found the best solution to be ecliptic coordinates λ = 290° ± 3° and β = –39° ± 2° (near the star alpha Pavonis), with an averaged sidereal period Ps = 0.610752 ± 0.000001 h. The uncertainty in λ, β, and sidereal period are chosen to be the mean standard deviation of the 49 single solution of the fine pole search. Since the ecliptic latitude of the rotations axis is negative, the asteroid has a retrograde rotation, i.e., it rotates clockwise when viewed from the ecliptic north pole. The study of the prograde-retrograde spin distribution of near-Earth asteroids is important, e.g., for the model of orbital drift of these bodies (La Spina et al., 2004). Of course this is a preliminary solution, but our confidence in the final solution is bolstered by the fact that the first half of the data gave only two possible solutions, one of which is the same solution using all data (Carbognani et al., 2016).

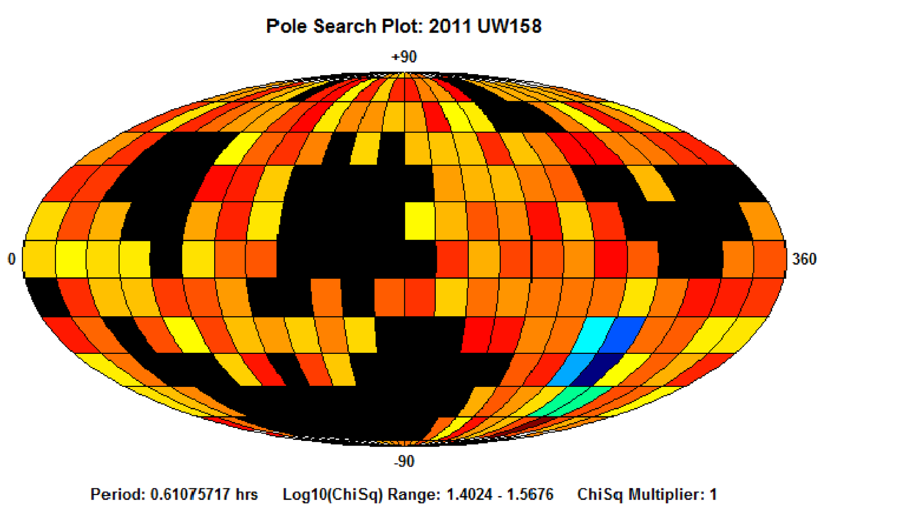

Figure 6 - Results of the "medium" pole search as a map of χ2 on the ecliptic sky. The deep blue region represents the pole location with the lowest Chi-square which increases as the color goes from light blue to green to yellow to orange and finally to deep red. Black regions indicate where the code produced an invalid result i.e. NAN, not a number (Carbognani et al., 2016).

Shape Model

The best shape model for this asteroid (the n. 24 in our data processing), shows a rather elongated object in rotation around the minor axis (Fig. 7). This result is consistent from the physical point of view and in agreement with the large LC amplitudes (>2 mag) found on some dates. This shape is also in agreement with the radar observations (Fig. 8). We tested the shape model by comparing synthetic lightcurves with observed ones. The shape model produces synthetic lightcurves that are in good agreement with observed lightcurves (Carbognani et al., 2016).

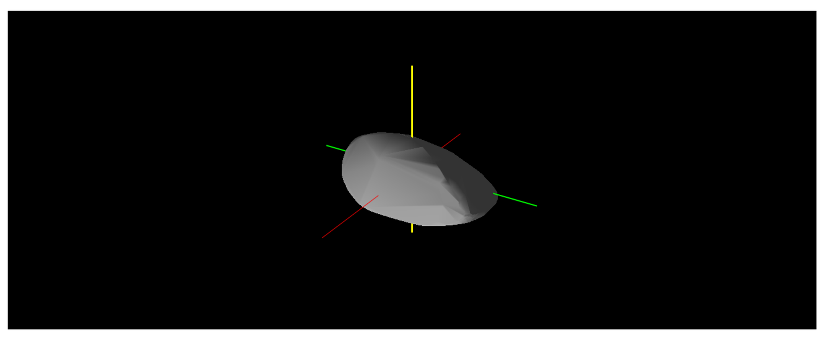

Figure 7 - The 3-D best model for 2011 UW158, with pole in λ = 295°, β = –40° (a/b=1.3, a/c=2.3, b/c=1.7).

Figure 8 - Delay-Doppler images of 2011 UW158 obtained on 2015 July 18 from Goldstone using SS-14 to transmit and Green Bank Telescope to receive. Resolution is 7.5 m x 5 Hz. Range increases down and Doppler frequency increases to the right. The images span a little more than 1 rotation of the object (Goldstone Radar Team; Naidu et al., 2015).

References

Belskaya, I. N., Schevchenko, V. G. (2000). "*Opposition Effect of Asteroids*." Icarus, **147**, 94-105.

Carbognani, A., Gary, B.L., Oey, J., Baj, G., Bacci, P. (2016). "*Pole and Shape for the NEA (436724) 2011 UW158*." Minor Planet Bulletin, **43**, 38-41.

Gary, B.L. (2016). "*Unusual Properties for the NEA (436724) 2011 UW158*.", Minor Planet Bulletin, **43**, 33-38.

Harris, A. W. (1997). "*On the Revision of Radiometric Albedos and Diameters of Asteroids*." Icarus, **126**, 450-454.

Holsapple, K.A. (2007). "*Spin limits of Solar System bodies: From the small fast-rotators to 2003 EL61*." Icarus, **187**, 500-509.

La Spina, A., Paolicchi, P., Kryszczynksa, A., Pravec P. (2004). "*Retrograde spins of near-Earth asteroids from the Yarkovsky effect*." Nature, **428**, 400-401.

Naidu, S.P. et al. (2015). "*Radar observations of near-Earth asteroid (436724) 2011 UW158 using the Arecibo, Goldstone, and Green Bank Telescopes*." American Astronomical Society, DPS meeting #47, id.204.08.

Kaasalainen, M., Torppa, J., Muinonen, K. (2001). "*Optimization methods for asteroid lightcurve inversion. II. The complete inverse problem*." Icarus, **153**, 37-51.

Kaasalainen, M., Torppa J. (2001). "*Optimization methods for asteroid lightcurve inversion. I. Shape determination*." Icarus, **153**, 24-36.

Pravec, P., Harris, A.W. (2000). "*Fast and Slow Rotation of Asteroids*." Icarus, **148**, 12-20.

Sànchez, P., Scheeres D.J. (2014). "*The Strength of Regolith and Rubble Pile Asteroids*." Meteoritics and Planetary Science, **49**, 788-811.

Schevchenko, V. G. (1997). "*Analysis of Asteroid Brightness-Phase Relations*." Solar System Research, **31**, 219-224.